

Atmospheric Optical CDMA Communication Systems via Optical Orthogonal Codes

Mahmoud Jazayerifar and Jawad A. Salehi, *Member, IEEE*

Abstract—We propose and consider using a class of multiple-access sequences, namely, optical orthogonal codes (OOCs) in atmospheric optical code-division multiple-access systems. We obtain analytical solutions to the error probability for various channel models using positive-intrinsic-negative diode and avalanche photodiode photodetectors. In our analysis, the effects of atmospheric turbulence, ambient light, thermal noise, and multiuser interference are considered, in the context of a semiclassical photon-counting approach. The performance of the systems taking advantage of space diversity and error-correcting codes are also evaluated. Two common and widely used optical modulations, on-off keying and pulse-position modulation, are considered. Receiver structures based on correlator and chip level are used for OOC detection. Unlike the traditional chip-level receiver, here a generalized form of chip-level structure with two threshold levels is considered. Upper and lower bounds on the error probability for the above-chip-level receiver structure is obtained. From our analytical results, we can deduce that the chip-level receiver outperforms a simple correlator in the absence or weak atmospheric fading; however, in a strong fading environment, the simple correlator outperforms the chip-level receiver.

Index Terms—Chip-level detector, free-space optical (FSO), optical code-division multiple access (OCDMA), scintillation, turbulence.

I. INTRODUCTION

ATMOSPHERIC or free-space optical (FSO) communication systems are receiving increasing attention for use in high-data-rate wireless links. These systems may be used as information bridges between buildings where there is no obstruction in the line-of-sight (LOS). They are cost-effective and easily installable, and lack of licensing requirements, as compared with microwave systems, is another advantage of these systems. Moreover, considering the narrow beamwidth used in these systems, they are also secure. Despite these advantages, optical communications through the air suffer from various atmospheric phenomena which causes a severe attenuation and fading [1], [5], [14].

Intensity modulation and direct detection (IM/DD) is the most viable information-bearing technique for atmospheric optical channels. On the other hand, optical orthogonal codes (OOCs) are also developed for code-division multiple-access (CDMA) systems using IM/DD [2]. In this paper, we consider

Paper approved by K. Kitayama, the Editor for Optical Communication of the IEEE Communications Society. Manuscript received June 25, 2005; revised February 5, 2006. This work was supported in part by the Iran National Science Foundation (INSF). This paper was presented in part at the International Symposium on Telecommunication (IST), Shiraz, Iran, September 2005.

The authors are with the Optical Network Research Laboratory (ONRL), Electrical Engineering Department, Sharif University of Technology, Tehran, Iran (e-mail: jazayerifar@ee.sharif.edu; jasalehi@sharif.edu).

Digital Object Identifier 10.1109/TCOMM.2006.881245

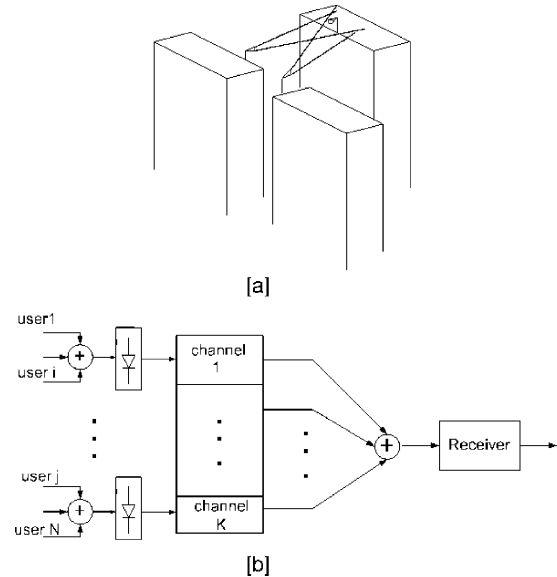


Fig. 1. (a) Buildings. (b) CDMA compound optical channel structure.

the performance of an atmospheric CDMA communications system using OOC codes. Based on the idea of minimizing the multiuser interference (MUI), different receiver structures for detection of OOCs, such as chip-level and hard-limiter, are proposed [3], [4]. In this paper, we consider a generalized form of chip-level receiver, and error-probability bounds for this generalized chip-level structure is obtained. In atmospheric optical CDMA (OCDMA) systems, various users may be placed either in the same location or in different locations. For example, they may be in one building or in different buildings, as sketched in Fig. 1(a). We call the case in which all of the users are placed in one location a single optical channel, and the case in which each user is placed in its own distinct location is a optical multichannel case. We also call the mixed case, in which users are divided into groups and various groups are placed in various locations, the compound optical channel. The block diagram of the compound channel structure is depicted in Fig. 1(b). Fading is one of the main factors affecting the performance of an atmospheric optical system, so some well-known techniques in communication systems, such as space diversity and error-correcting codes, can improve the performance considerably. Optical amplifiers (OAs) and avalanche photodiodes (APDs) also improve the performance, if the received power level is low in comparison with thermal noise. Both 850 nm and 1.55 μm wavelengths can be used. 850 nm photodetectors are more sensitive than 1.55 μm photodetectors, however, erbium-doped fiber amplifiers (EDFAs) operate at 1.55 μm .

Therefore, they can be used in atmospheric systems, provided that $1.55 \mu\text{m}$ is used. In this paper, we consider $1.55 \mu\text{m}$. In order to obtain analytical solutions to the error probability, we use the Gaussian approximation method, conditioned on the fading level. Due to the dominance of thermal noise, this method is considered to be accurate. Prior to this paper, some other papers on atmospheric OCDMA systems were presented in [12] and [13]. In [12], the systems using OOCs are compared with systems using Walsh–Hadamard codes. In [13], the performance of the systems using pulse-position modulation (PPM) in a multichannel structure are evaluated. In this paper, we consider a more general assumption, and evaluate the performance of various structures.

The rest of this paper is organized as follows. In Section II, our system models, channels, transmitters, and receivers will be discussed. In Section III, performance of the proposed OCDMA systems will be evaluated. In Section IV, some typical techniques in communication will be used in order to improve the performance, and finally, in Section V, numerical results will be presented.

II. SYSTEM DESCRIPTION

A typical narrowbeam LOS atmospheric optical communication system consists of three parts: transmitter, channel, and receiver. In this section, we study these three parts in the context of our proposed OCDMA systems.

A. OCDMA Transmitter

It is assumed that transmitter is equipped with a laser diode operating at wavelength λ . The mean photon counts of the transmitted pulses representing zero and one are, respectively, $m_{t,0,c} = 0$ and $m_{t,1,c} = P_{t,1}T_c/h\nu$, where $P_{t,1}$, T_c , ν , and h are the peak transmitted power, chip duration, optical frequency, and Planck's constant, respectively. The OOC is characterized by its length F , the number of chips, and its weight w , the number of chips that may be one or zero, depending on the value of transmitted data bit. We consider two types of modulations, namely on–off keying (OOK) CDMA and PPM CDMA. In OOK signaling, a pulse “1”(“0”) represents a data bit “0”(“1”). OOK CDMA signaling is obtained by multiplication of OOK signals by OOC. Considering the transmitted signal in OOK CDMA that represent data bit “1,” we can construct the binary (B)PPM CDMA signaling scheme as follows. We divide the duration of each chip T_c into two parts, and send a pulse “1”(“0”) in the first part, followed by a pulse “0”(“1”) in the second part to represent a data bit “0”(“1”). Considering these notations for BPPM, $m_{t,0,c}$ represents the mean photon count in the first part of the chip, and $m_{t,1,c}$ represents that in the second part of the chip.

B. Atmospheric Optical Channel

Atmospheric channel parameters vary depending on the air condition. For example, the channel attenuation in hazy weather is more than that in clear weather. Here, we consider attenuation, fading, and ambient light in the clear-air condition. Channel attenuation is caused by both molecular absorption and aerosol

scattering, as well as beam divergence. The total channel attenuation is equal to [5]

$$a = \frac{A}{\pi \left(\frac{\Theta L}{2}\right)^2} e^{(-\beta L)} \quad (1)$$

where β , L , A , and Θ are, respectively, atmospheric extinction coefficient, the length of the link, the area of the optical receiver, and the angle of divergence in radians. The atmospheric optical channel fading is caused by random refractive-index variations. This fading is modeled as a multiplicative normalized log-normal random variable [5]. Therefore, considering the linear relationship between power and count, the received photon count can be related to the transmitted photon count as follows:

$$m_{r,d,c} = ae^{2x} m_{t,d,c} \quad d = 0 \text{ or } 1 \quad (2)$$

where $m_{t,d,c}$ is the mean number of transmitted photons, and $m_{r,d,c}$ is the mean number of received photons, index d represents the value of the transmitted pulse, and the probability density function (PDF) of x is as follows:

$$f(x) = \frac{1}{(2\pi)^{1/2}\sigma_x} e^{-(x+\sigma_x^2)^2/2\sigma_x^2} \quad (3)$$

where $\sigma_x^2 = \min(0.124K^{7/6}C_n^2L^{11/6}, 0.5)$ and $K = 2\pi/\lambda$ is the wave number at the operating wavelength λ , L is the path length, and C_n^2 is the refractive index structure constant [5]. Note that the mean of x is $-\sigma_x^2$, which makes the fading normalized so that $E(e^{2x}) = 1$, and consequently, $E(ae^{2x}) = a$. Coherence time of this fading is typically on the order of milliseconds, and coherence length is typically on the order of millimeters [5]. Another characteristic of optical wireless channel is its ambient light. The mean number of ambient photons in a time interval with duration T_c is as follows:

$$m_{a,c} = \frac{W(\lambda)A\Omega_{\text{FOV}}\Delta\lambda T_c}{h\nu} \quad (4)$$

where Ω_{FOV} is the receiver field of view (FOV) in stradian, $\Delta\lambda$ is the optical filter bandwidth, and $W(\lambda)$ is the spectral radiance function, defined as the power radiated at wavelength λ per cycle of bandwidth in a unit solid angle per unit of source area. Because of the narrow field in atmospheric systems, $m_{a,c}$ is usually very weak, especially in comparison with that of nondirected wireless optical indoor systems.

C. Various Receiver Structures

A typical optical wireless receiver consists of a lens which focuses the received optical field on a photodetector, where this photodetector can be a positive-intrinsic-negative diode (PIN), an APD, or a PIN coupled to an OA. It is well known that due to the existence of the ambient light, the photon count of the received optical signal has a Laguerre PDF. As we discussed in Section II-B, ambient light is usually very weak. Therefore, this

Laguerre distribution can be approximated by a Poisson distribution [6]. After photodetection, the released electrical current will be added with a zero-mean Gaussian thermal noise caused by the electrical circuit. The variance of the electron count produced by thermal noise is equal to

$$\sigma_{th,c}^2 = \frac{2K_b T_r T_c}{Re^2} \quad (5)$$

where K_b is Boltzman's constant, T_r and R are the receiver equivalent temperature and load resistance, respectively, and e is the electron charge. Hereby, we obtain the mean and the variance of the electron count for various photodetectors for our various optical receiver structures.

1) *PIN*: If we represent the quantum efficiency by η and dark current by i_d , the mean and variance of the released electron count is equal to [6]

$$\text{mean(PIN, } d, c) = \eta(m_{r,d,c} + m_{a,c}) + m_{dcu,c} \quad (6)$$

$$\text{var(PIN, } d, c) = \text{mean(PIN, } d, c) + \sigma_{th,c}^2 \quad (7)$$

where $m_{dcu,c} = i_d T_c / e$ is the dark current electron count in a chip duration (T_c).

2) *APD*: APD can improve the performance by increasing the received signal level relative to the additive thermal noise. We consider an APD with gain G , noise factor ξ , quantum efficiency η , bulk leakage current I_b , and surface leakage current I_s . Considering dark currents and thermal noise, the mean and the variance of the electron count will be as follows [6]:

$$\text{mean(APD, } d, c) = G\eta(m_{r,d,c} + m_{a,c}) + \frac{T_c I_s}{e} + \frac{G T_c I_b}{e} \quad (8)$$

$$\begin{aligned} \text{var(APD, } d, c) &= [G\eta(m_{r,d,c} + m_{a,c})]^2 (\xi - 1) + \frac{T_c I_s}{e} \\ &+ \frac{G^2 T_c I_b \xi}{e} + \sigma_{th,c}^2. \end{aligned} \quad (9)$$

3) *Optical Amplifier (OA)*: We consider an EDFA. We assume that the receiver optics can couple the received field into an OA with gain G and noise factor $K = n_{sp}(G - 1)$, where n_{sp} is the spontaneous emission parameter. We also represent the number of spontaneous modes of the OA with D . After the OA, a PIN is installed. Considering a Poisson distribution for the number of applied photons to the OAs, the PDF of the number of output photons is a Laguerre distribution with mean $G\eta(m_{r,d,c} + m_{a,c}) + DK\eta$ and variance $G\eta(m_{r,d,c} + m_{a,c})(1 + 2K\eta) + D(\eta K + (\eta K)^2)$ [11]. Considering dark current and thermal noise, the mean and the variance of the number of electrons released will be as follows:

$$\text{mean(OA, } d, c) = G\eta(m_{r,d,c} + m_{a,c}) + DK\eta + m_{dcu,c} \quad (10)$$

$$\begin{aligned} \text{var(OA, } d, c) &= G\eta(m_{r,d,c} + m_{a,c})(1 + 2K\eta) \\ &+ D(\eta K + (\eta K)^2) + m_{dcu,c} + \sigma_{th,c}^2. \end{aligned} \quad (11)$$

After photodetection, the received signal is multiplied by the OOC. After this step, there are various approaches to make a decision on the transmitted bit which lead to various receiver structures. Here, we consider two structures, namely, a simple correlator and a chip-level detector.

4) *Correlator*: In this structure, the detection of OOK signals is made as follows. The photodetected signal is first multiplied by its corresponding OOC, integrated over one bit ($T = FT_c$), and finally compared with a constant threshold to make the final decision. On the other hand, in BPPM signaling, the corresponding OOC chips are divided into two parts: the first part corresponding to the "0" data bit, and the second part corresponding to the "1" data bit. The decision on the value of the received bit is made by comparing the integrated photodetected signal in each part. On the other hand, the coherence time of fading is on the order of several milliseconds [5], [14], while usual bit durations are less than several microseconds; therefore, we can assume that the fading is constant during a bit period with a very good approximation. Considering the structure of correlator receiver, independence of counts for different chip intervals, and the fact that the fading is approximately constant during a bit period, we can write

$$\text{mean(det, } d, b) = \sum_{i=1}^w \text{mean}_i(\text{det, } d, c) \quad (12)$$

$$\text{var(det, } d, b) = \sum_{i=1}^w \text{var}_i(\text{det, } d, c) \quad (13)$$

where $\text{mean}_i(\text{det, } d, c)$ is the mean electron count of the i th chip pulse interval of the corresponding OOC, b represents that this mean and variance are the mean and variance of bit count (not chip count), "det" represents the photodetector (PIN, APD, or OA), and w is the weight of OOC.

5) *Chip Level*: The main advantage of this receiver structure over correlator structure is that it is more resistant to the MUI. This receiver structure is mainly proposed for OOK signaling [4]. In this structure, after multiplication of the photodetected signal by the corresponding OOC, a primary decision is made on the value of each chip (by comparing the integration of the received signal over a chip duration with a constant threshold), followed by a final decision by comparing the number of ones and zeros produced by primary decisions with a constant threshold, which is a number between one and w . In [4], the threshold value is considered to be fixed and equal to w , which is the optimum threshold if the only source of error is MUI, but in atmospheric systems, there are several other sources of error. Changing the threshold value may lead to better performance, so, in this paper, we use a generalized chip-level receiver structure with a threshold which may be any value between one and w .

III. ANALYSIS OF ATMOSPHERIC OCDMA SYSTEMS

In Section III, we discuss the performance of correlator and chip-level structures for detection of OOCs in the context of atmospheric optical systems. We obtain analytical solutions of the error probability for these receiver structures.

A. Correlator

As discussed before, there are several structures for atmospheric OCDMA channels. Here, we consider the compound channel which is the general case. Other channel structures can be considered as the special cases of this structure. Considering the multiple-access interference, in the j th chip, the mean

number of photons transmitted by the group containing the desired user equals $m_{t,d,c} + r_1^{(j)} m_{t,1,c}$, where $r_1^{(j)}$ is the number of interfering users of the group containing the desired user. Considering (2), we obtain the photon count of the received signal

$$m_{r,d,c}^{(1,j)} = (m_{t,d,c} + r_1^{(j)} m_{t,1,c}) a_1 e^{2x_1} \quad (14)$$

where the superscript (1) represents the first group of users, and (j) represents that this count corresponds to the jth chip ($1 \leq j \leq w$). Other groups also cause the interfering pulses with photon count $r_i^{(j)} m_{t,1,c}$, where $r_i^{(j)}$ is the number of interfering users of group i . Considering (2) for group i , we have

$$m_{r,d,c}^{(i,j)} = r_i^{(j)} m_{t,1,c} a_i e^{2x_i}. \quad (15)$$

Different group signals have passed through different channels, and as a result, they are affected by independent fading. The electron counts of different chips with mean $m_{r,d,c}^{(i,j)}$ are also independent because they are counts of different times. Therefore, the total received photon count is obtained by use of (15) and (14)

$$m_{r,d,c}^{(j)} = (m_{t,d,c} + r_1^{(j)} m_{t,1,c}) a_1 e^{2x_1} + \sum_{i=2}^M (r_i^{(j)} m_{t,1,c}) a_i e^{2x_i} \quad (16)$$

where M is the total number of groups. By substituting (16) in (6) to (11), we can obtain the mean and the variance of the number of electrons in each chip for different photodetector. For example, for a PIN, we have

$$\begin{aligned} \text{mean(PIN, } d, c) &= \eta(m_{t,d,c} + r_1^{(j)} m_{t,1,c}) a_1 e^{2x_1} \\ &+ \sum_{i=2}^M (r_i^{(j)} m_{t,1,c}) a_i e^{2x_i} + \eta m_{a,c} + m_{d,c}. \end{aligned} \quad (17)$$

And finally, by considering (12), (13), and (17), we obtain the mean and variance of decision variable

$$\begin{aligned} \text{mean(PIN, } d, b) &= \eta(m_{t,d,c} w + l_{1,1} m_{t,1,c}) a_1 e^{2x_1} \\ &+ \eta \sum_{i=2}^M l_{i,1} m_{t,1,c} a_i e^{2x_i} + w m_{a,c} \eta + w m_{d,c}. \end{aligned} \quad (18)$$

$$\text{var(PIN, } d, b) = \text{mean(PIN, } d, b) + w \sigma_{th,c}^2 \quad (19)$$

where l_i is the total number of interferences caused by the i th group users in a period (T) ($l_i = \sum_{j=1}^w r_i^{(j)}$). Therefore, we can obtain the error probability using the Gaussian approximation method as follows.

1) *OOK Modulation*: Conditional error probability can be written as

$$P(e|\vec{l}, \vec{X}, 0) = Q\left(\frac{\text{Th} - \text{mean(PIN, 0, } b)}{\sqrt{\text{var(PIN, 0, } b)}}\right) \quad (20)$$

$$P(e|\vec{l}, \vec{X}, 1) = Q\left(\frac{\text{mean(PIN, 1, } b) - \text{Th}}{\sqrt{\text{var(PIN, 1, } b)}}\right) \quad (21)$$

where $\vec{l} = (l_1, l_2, \dots, l_M)$, $\vec{X} = (x_1, x_2, \dots, x_M)$, and $Q(x) = \int_x^\infty 1/(\sqrt{2\pi}) e^{-(x^2/2)} dx$. The error probability is obtained by averaging with respect to \vec{l} and \vec{X}

$$P(e|\vec{X}, d) = \sum_{l_1 + \dots + l_M < N} P(e|\vec{l}, \vec{X}, d) Pr(\vec{l}) \quad (22)$$

where N is the number of users, d represents the data and may be 1 or 0, and $Pr(\vec{l})$ is obtained by generalization of $Pr(l)$ in [2]

$$\begin{aligned} Pr(\vec{l}) &= \binom{N_1 - 1}{l_1} \prod_{i=2}^M \binom{N_i}{l_i} q^{\sum_{i=1}^M l_i} (1 - q)^{\sum_{i=1}^M N_i - \sum_{i=1}^M l_i - 1}, \\ q &= \frac{w^2}{2F} \end{aligned} \quad (23)$$

where F is the OOC length, and $\binom{b}{a} = b! / a!(b - a)!$. Finally, we can write

$$Pe = \frac{1}{2} \int_{\vec{X}} (P(e|\vec{X}, 0) + P(e|\vec{X}, 1)) f(\vec{X}) d\vec{X} \quad (24)$$

where $f(\vec{X}) = \prod_{i=1}^M f(x_i)$ and $d\vec{X} = \prod_{i=1}^M dx_i$. In the above equations, we have considered a constant threshold level. However, by considering (18)–(19), we notice that the mean and variance of the decision variable is related to the fading level (x_i). On the other hand, we know that the optimum threshold is a function of the mean and variance of the received signal, so instead of using a constant threshold, it is preferable and more appropriate to use an adaptive threshold, varying according to fading level. We assume that the receiver is equipped with an estimator, so that when it receives data bits, the channel is already estimated perfectly [15]. Fortunately, due to the slow fading, the value of x_1 , and, as a result, the optimum threshold, can be adaptively estimated. This optimum threshold ($Th(x)$) can be obtained either by computer search or by solving the equation $\partial P(e|\vec{X}) / \partial Th = 0$. However, an alternative approach, in order to avoid having to evaluate for the optimum threshold, is to use BPPM.

2) *BPPM*: Contrary to OOK modulation, in BPPM signaling, interference due to interfering users transmitting binary zero affect the error probability. When $l_{1,i}$ interfering users of group i transmit bit zero, and $l_{2,i}$ interfering users transmit bit one, the mean of the decision variable for each half-bit of BPPM signaling is as follows:

$$\begin{aligned} \text{mean(PIN, } d, b) &= (m_{t,d,c} w + l_{1,1} m_{t,1,c}) \eta a_1 e^{2x_1} + \\ &+ \sum_{i=2}^M (l_{1,i} m_{t,1,c}) a_i e^{2x_i} \eta + w \eta m_{a,c} + w m_{d,c}. \end{aligned} \quad (25)$$

$$\begin{aligned} \text{mean(PIN, } 1 - d, b) &= (m_{t,1-d,c} w + l_{2,1} m_{t,1,c}) \eta a_1 e^{2x_1} + \\ &+ \sum_{i=2}^M (l_{2,i} m_{t,1,c}) a_i e^{2x_i} \eta + w \eta m_{a,c} + w m_{d,c}. \end{aligned} \quad (26)$$

and the variance for each half-bit of BPPM signaling is obtained by substituting (25) or (26) in (19). Conditional error probability is

$$P(e|\vec{l}_1, \vec{l}_2, \vec{X}) = Q \left(\frac{\text{mean}(\text{PIN}, 1, b) - \text{mean}(\text{PIN}, 0, b)}{\sqrt{\text{var}(\text{PIN}, 1, b) + \text{var}(\text{PIN}, 0, b)}} \right). \quad (27)$$

By averaging with respect to $\vec{l}_1 = (l_{1,1}, \dots, l_{1,M})$ and $\vec{l}_2 = (l_{2,1}, \dots, l_{2,M})$, we will have

$$P(e|\vec{X}) = \sum_{\text{sum}(\vec{l}_1) + \text{sum}(\vec{l}_2) < N} P(e|\vec{l}_1, \vec{l}_2, \vec{X}) Pr(\vec{l}_1, \vec{l}_2) \quad (28)$$

and

$$Pr(\vec{l}_1, \vec{l}_2) = \binom{N_1 - 1}{l_{1,1}, l_{2,1}} \times \prod_{i=2}^M \binom{N_i}{l_{1,i}, l_{2,i}} q^{\sum_{i=1}^M (l_{1,i} + l_{2,i})} (1 - 2q)^{\sum_{i=1}^M (N_i - (l_{1,i} + l_{2,i})) - 1} \quad (29)$$

where $\text{sum}(\vec{l}_i) = \sum_{j=1}^M l_{i,j}$ with $i = 1$ or 2 . Finally, the error probability is obtained by substituting (28) in (24).

B. Chip Level

In the previous section, we considered the general channel structure. Here, we consider the single channel structure. Using a constant-threshold OOK receiver, the electron count of each chip is compared with the threshold, so assuming that the desired user transmits zero, if no interference occurs in a chip, the error probability for that chip will be equal to $P_0 = Q(\text{Th-mean}(\text{PIN}, 0, c) / \sqrt{\text{var}(\text{PIN}, 0, c)})$. Similarly, $P_1 = Q(\text{Th-mean}(\text{PIN}, 1, c) / \sqrt{\text{var}(\text{PIN}, 1, c)})$ and $P_2 = Q(\text{Th-mean}(\text{PIN}, 2, c) / \sqrt{\text{var}(\text{PIN}, 2, c)})$ will be the error probability for the chips interfered by one and two interferences, respectively, where $\text{mean}(\text{PIN}, 0, c)$, $\text{mean}(\text{PIN}, 1, c)$, and $\text{mean}(\text{PIN}, 2, c)$ are defined according to (17), by substituting $(d = 0, r_1 = 0)$, $(d = 1, r_1 = 0)$, and $(d = 1, r_1 = 1)$ for $M = 1$, respectively. It can also be observed that assuming the desired user transmits one, the chip-error probability will be equal to $1 - P_1$ and $1 - P_2$ if zero and one interference occurs, respectively. Now, considering the above chip-error probabilities, we can obtain the upper $P_U(e|x)$ and lower $P_L(e|x)$ bounds on the bit-error probability conditioned on the fading level (Appendix). Finally, upper and lower bounds of the error probability are obtained by averaging the above bounds with respect to x . In the above discussion, we considered a constant threshold receiver. But we can also use an adaptive threshold receiver to improve the system performance for the chip-level detection scheme.

IV. METHODS FOR IMPROVING THE PERFORMANCE

In this section, we consider some well-known methods in order to improve the performance of the system.

A. Error-Correcting Codes

The super orthogonal code (SOC) used in this paper is exactly the same as the one used in [9]. The prime reason in using SOC is due to its simple encoder and decoder structures. The constraint length is K , and the output rate is 2^{K-2} times the input bit rate. Either hard decoding or soft decoding can be used for decoding of SOC. Soft decoding usually outperforms hard decoding. In hard decoding, a primary decision is made on the value of each chip, and then using Viterbi algorithm, the final decision on the transmitted bit stream is made. In this paper, we only consider hard decoding. For multiple-access usage, we must combine OOC and SOC. It can be simply done in a way which does not impose any bandwidth expansion [9]. In this method, output bits of the encoder are respectively located in OOC weight positions. Therefore, the rate of SOC must be equal to OOC weight ($w = 2^{K-2}$). The generating function of the SOC is computed in [9] as

$$T(z, b) = \frac{bG^{K+2}(1-G)}{1-G[1+b(1+G^{K-3}-2G^{K-2})]} \quad (30)$$

in which $G = z^{2^{K-3}}$. If we use interleaving in conjunction with coding, the channel becomes memoryless, and we can simply obtain the upper bound on the error probability, but using interleaving is not implementable, since the fading is very slow. We consider a single-channel structure. If we do not use the interleaving, electron counts of different chips will be independent only if they are conditioned on the fading level. The fading is slow enough to be considered constant. Finally, conditioning on fading level, we can write

$$P(e|x) < \frac{\partial T(z, b)}{\partial b} \Big|_{b=1} = \frac{G_{|x}^{K+2}}{(1-2G_{|x})^2} \left(\frac{1-G_{|x}}{1-G_{|x}^{K-2}} \right)^2 \quad (31)$$

where $G_{|x} = z_{|x}^{2^{K-3}}$, $z = \sqrt{P(e|0, x)(1-P(e|1, x)) + \sqrt{P(e|1, x)(1-P(e|0, x))}}$. $P(e|0, x)$ and $P(e|1, x)$ are obtained by substituting $\text{mean}(\text{PIN}, d, b)$ with $\text{mean}(\text{PIN}, d, c)$ and following (20) to (22), where $q = w/2F$ and $M = 1$. Finally, the error probability is obtained by averaging (31) with respect to x . For PPM signaling, a similar equation to (17) for mean electron count in each chip can be obtained. Again, by substituting $\text{mean}(\text{PIN}, d, b)$ and $\text{mean}(\text{PIN}, 1-d, b)$ with $\text{mean}(\text{PIN}, d, c)$ and $\text{mean}(\text{PIN}, 1-d, c)$, setting $q = w/2F$ and following (27) to (29), $P(e|1) = P(e|0)$ is obtained.

B. Space Diversity

In this section, we consider one transmitter and D receivers with equal areas, so that the distances between the receivers are larger than the coherence length. We use a linear combining method with constant identical coefficients, which leads to a simple adder structure, since other coefficients do not improve the performance significantly [10]. Considering the OOK signaling and correlator receiver, the electron count received from

TABLE I
VALUES USED FOR NUMERICAL RESULTS

Parameter	value
R (bit rate)	10 Mbit/s
λ (wave-length)	1.55 μm
P_t (transmitted power)	0.4 mW
w (code weight)	8
F (code length)	400
N (number of users)	6
i_d (PIN) (dark current)	5 nA
i_s (APD) (surface dark current)	10 nA
i_b (APD) (bulk dark current)	0.1 nA
R (resistance)	10 K Ω
η (quantum efficiency)	0.8
$\Delta\lambda$ (optical filter bandwidth)	1 nm
Θ_{FOV} (field of view angle)	5 mrad
D_{lense} (lens diameter)	6 cm
$W(\lambda)$ (special radiance function (day time))	$10^{-3} \frac{w}{\text{cm}^2 - \mu\text{m} - \text{sr}}$
$D_{photo-det}$ (photo-detector diameter)	1 μm
G_{EDFA} (gain of optical amplifier at λ)	1000(30dB)
n_{sp} (spontaneous emission parameter)	1
T_r (temperature)	300 K
G_{APD} (gain of APD) at λ	10
L (channel length)	3 Km
β (attenuation coefficient for clear air)	0.1 K m^{-1}

each diversity path is obtained according to (18). The mean of the decision variable is

$$\begin{aligned} \text{mean(PIN, } d, b) &= \eta a_1 (m_{t,d,c} w + l_1 m_{t,1,c}) \\ &\times \sum_{j=1}^D e^{2x_{1,j}} + \sum_{j=1}^D \sum_{i=2}^M l_i m_{t,1,c} a_i e^{2x_{i,j}} \eta \\ &+ \eta D w m_{a,c} + D w m_{dcu,c}. \end{aligned} \quad (32)$$

Using the Wilkinson approximation [7], we can substitute $\sum_{j=1}^D e^{2x_{i,j}}$ with e^{y_i} , where y_i is a Gaussian random variable with variance $\sigma_{y_i}^2 = \ln((\exp(4\sigma_{x_i}^2) - 1) + D)/D$ and the mean $\ln D - \sigma_{y_i}^2/2$. By substituting $2x$ with y and following (20) to (24), the error probability can be obtained. For PPM signaling, the mean and variance of the decision variable and, consequently, the error probability, can be obtained in a similar fashion.

V. NUMERICAL RESULTS

In this section, we present numerical results on the performance of various systems. For clarity in showing the curves, we use the following abbreviated words, such as, ‘‘cc, mc, sc, adp th, cte th, coltr, chp lvl, bnd, and div’’ which correspond to ‘‘compound channel, multichannel, single channel, adaptive threshold, constant threshold, correlator, chip level, error-probability bound, and space diversity,’’ respectively. In Table I, the nominal values for system parameters used in this section are listed. For these values, using (1), the received power is $P_r = 5$ nW, and the corresponding mean photon count is $m_{r,d,c} = P_r T_b / h\nu w = 488$. Also, $\sigma_{th}^2 = 8086$ and $m_{a,c} = 3 \times 10^{-5}$ according to (5) and (4). The photodetector used in most figures is PIN. Code length, bit rate, and peak power are kept constant when comparing OOK versus PPM; therefore, in our numerical results, the bandwidth for BPPM is twice as much as that

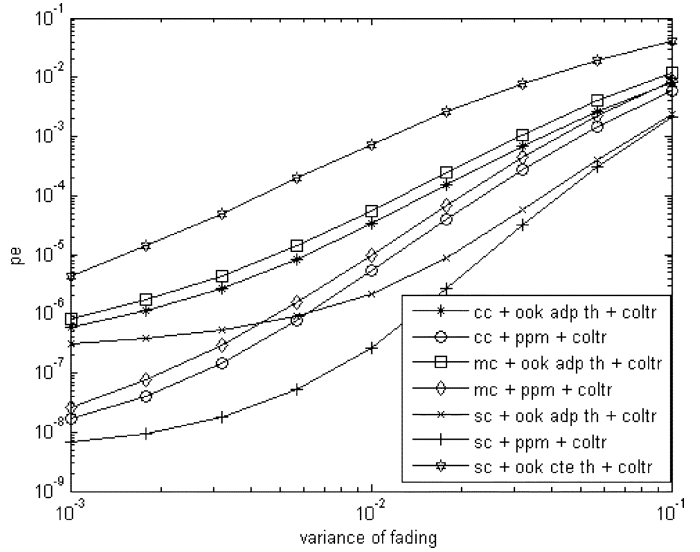


Fig. 2. Error probability of different channel structures and different modulations versus fading level.

of OOK, and the OOK mean photon count is twice as much as the BPPM count, since the chip duration in BPPM is half the chip duration of OOK. We also assume that in the compound channel structure, users are divided into two groups, each containing $N/2$ users.

Fig. 2 shows the error probability of different structures. First of all, we observe that the system using OOK modulation with constant threshold has the worst performance. Also, single channel has the best performance among other structures. Through an example, we clarify why the single-channel structure outperforms other optical channel structures. Consider PPM signaling. Assume that the desired user transmits one pulse in the first time slot corresponding to the zero bit, and assume that this pulse is strongly attenuated by fading. On the other hand, other transmitters may transmit pulses interfering in other time slots, so that these pulses are not strongly attenuated by fading. In such a condition, an erroneous decision is very likely. But this condition can not take place in the single-channel structure, because in this structure, all users are affected by the same fading level. We also note that the error probability of multichannel and compound channel structures are very close. In Fig. 3, the same error probabilities are depicted versus the variance of thermal noise.

In Fig. 4, the performance of correlator and chip-level receivers in a single-channel structure is shown. OOK modulation is considered. As expected, the adaptive threshold method outperforms constant threshold. From this figure, we can conclude that chip level outperforms correlator, especially for low values of fading variance. The reason is that when fading is weak, the effect of MUI on the error probability becomes apparent. Therefore, the chip-level receiver, which is more resistant to MUI, outperforms the correlator receiver. For large values of fading variance, the dominant source of error is fading. In this circumstance, the correlator using the adaptive threshold method outperforms chip-level using adaptive threshold. The reason is

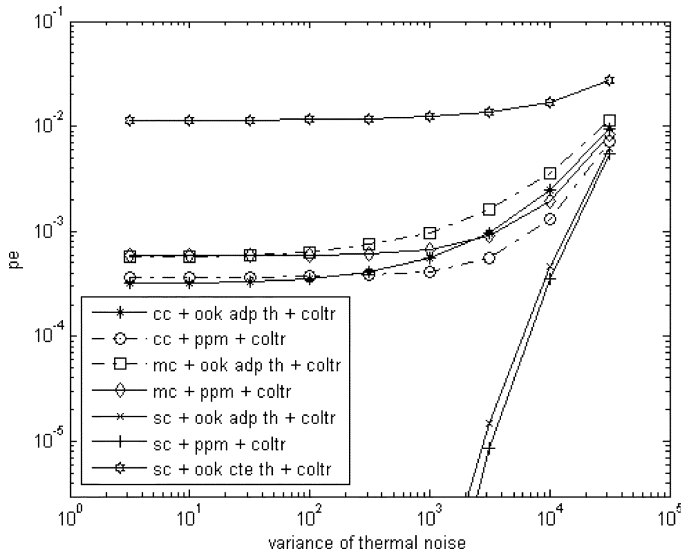


Fig. 3. Error probability of different channel structures and different modulations versus variance of thermal noise.

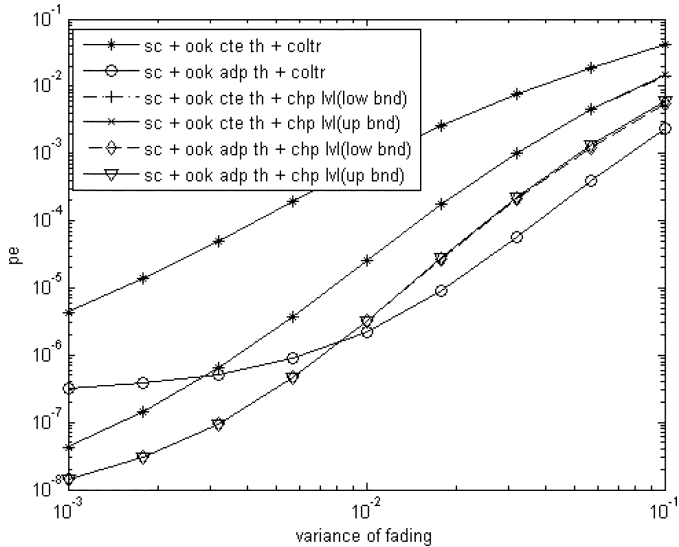


Fig. 4. Error probability of correlator and chip-level receivers versus fading variance.

that unlike the chip-level receiver in which every chip is detected and decided separately, in the correlator receiver, the received signal of different chips are first added before comparing with the threshold value. This addition reduces the effect of noise and fading. Also, we further note that the error-probability bounds obtained for the chip-level receiver are very tight. In Fig. 5, the performance of correlator and chip-level receivers in a single-channel structure versus the variance due to thermal noise is shown. Once again, we can observe that the performance of the correlator receiver intersects that of chip level for the adaptive threshold case. This can be reasoned as we discussed for Fig. 4. Note that from Fig. 5, the constant threshold correlator is very sensitive to fading, and the fading level is the same for

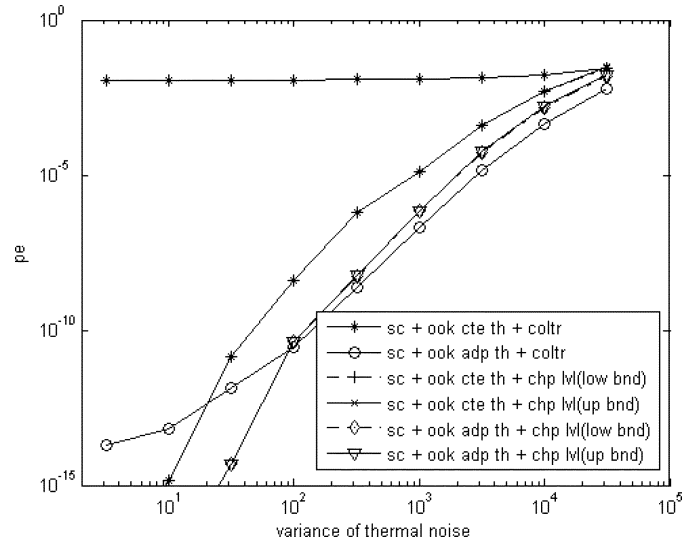


Fig. 5. Error probability of correlator and chip-level receivers versus the variance of thermal noise.

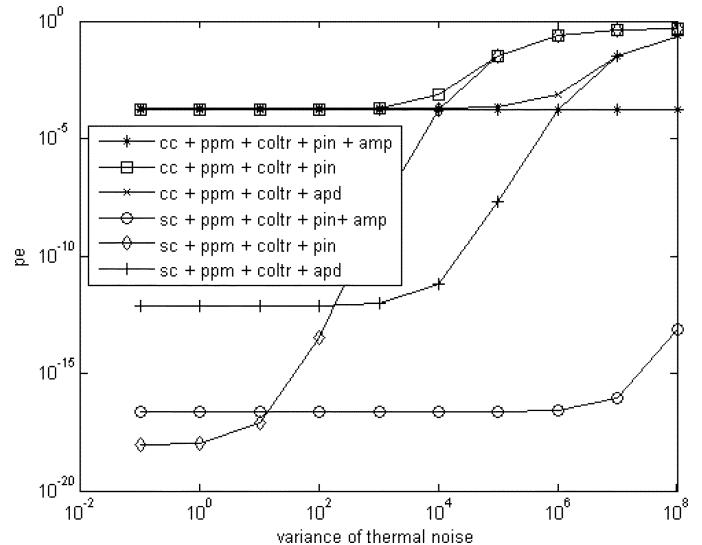


Fig. 6. Error probability of systems using PIN, APD, and PIN + EDFA versus thermal noise variance.

all points and dominant for this receiver, so the performance of this system remains at a constant value.

In Fig. 6, the error probabilities for systems using PIN, APD, and OAs versus the variance due to thermal noise are shown. We consider single channel and compound channel structures. Considering single-channel plots, we observe that for low values of thermal noise, PIN outperforms APD, because detectors are shot-noise limited and the effect of excess noise of APD and OA is apparent. But for higher values of thermal noise variance, the received signal level becomes comparable to additive thermal noise, so those detectors that amplify the received signal, i.e., APD and OA, outperform PIN. As it can be seen from Fig. 6, the performance of systems using APD is always worse than the performance of systems using OAs, since the gain of APD is, by far, lower than OA while its noise is not less than OA. Note that for almost all cases, some floor values occur. The reason is that

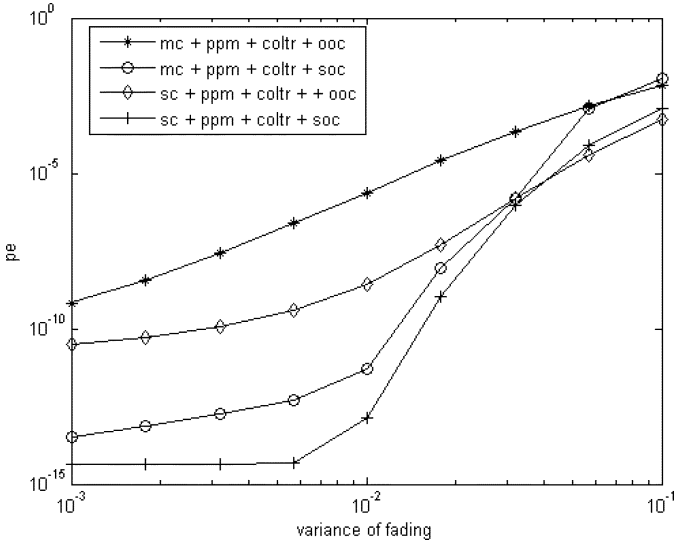


Fig. 7. Error probability of systems using SOC versus fading variance.

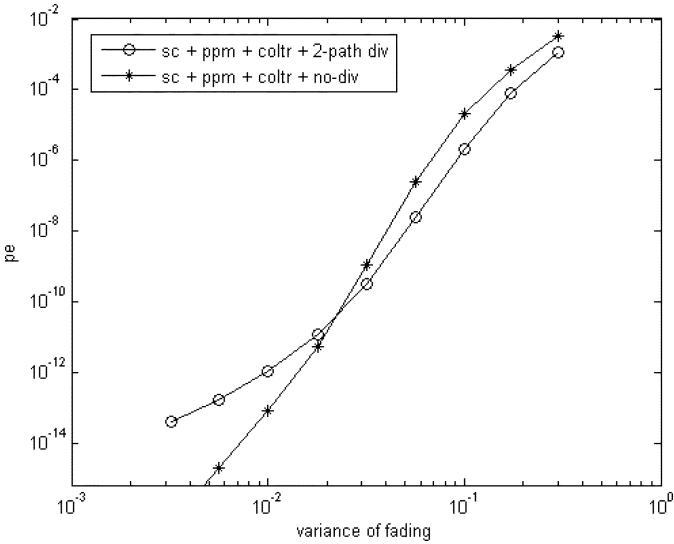


Fig. 8. Error probability of the system using space diversity versus fading variance.

when the variance of thermal noise decreases, one of the other sources of error, such as MUI or excess noise of APD or OA, become the dominant source of error, and their corresponding value remains the same for all points on the curve. Note that the floor value for the compound channel case is approximately the same for all photodetectors due to fading dominance.

In Fig. 7, we consider the performance of a system using SOC without interleaving using PPM. For large values of fading variance, the performance of the systems using SOC is approximately the same as the systems using OOC. That is because of the slow fading, which results in burst-mode errors. In fact, in order to achieve an appropriate performance, coding must be used in conjunction with interleaving, but since the fading is very slow, it leads to a very deep interleaver which is not implementable. In Fig. 8, we consider a system using space diversity. We compare the performance of two systems. One system

consists of a big receiver lens, and the other consists of two receiver lenses with an area for each being half of the area of the first system's lens. We assume that the distance between these lenses is larger than the coherence length of the channel. As it can be seen, for large values of fading, the system using space diversity outperforms the system not using it. For low values of fading, the thermal noise becomes the dominant source of error. The noise level of the system using two receivers is twice as much as the system using one receiver, so for low values of fading, the system using one receiver outperforms the system using two receivers.

VI. CONCLUSION

In this paper, various receiver structures used in a typical atmospheric OCDMA system are studied. We observed that chip level usually outperforms receivers based on correlator. We also compared various channel structures, and noted that single channel outperforms other structures. Subsequently, we used space diversity and coding to mitigate the effect of fading. We also used OAs and APDs to suppress the effect of thermal noise. We noticed that APD and OAs improve the system performance. PPM usually outperforms OOK, but the main disadvantage of PPM is its excess bandwidth. Using space diversity can also improve the performance. Since the coherence length of the atmospheric channel usually is on the order of centimeters, space diversity can be easily implemented.

APPENDIX

In this appendix, we obtain error-probability bounds for a single-channel structure and OOK signaling. Here, we derive the error probability for systems where the number of users is less than the code weight. In the chip-level receiver, after detecting chips separately, the number of "1" detected chips is compared with TH ($w \geq TH \geq 1$) and if it is larger than TH , bit "1" is declared, otherwise "0" is declared. For simplicity, we define $TH0 = \lfloor TH \rfloor + 1$ and $TH1 = w - \lfloor TH \rfloor$. The main idea for obtaining upper and lower bounds is to make the error probability conditioned on the number of chips affected by interference. In the first step, the error probability is made conditioned on the number of occurred interferences (l). We know that the probability of occurrence of l interferences in one period is obtained according to (23). For the single-channel structure, \vec{l} simplifies to a scalar value l . So, assuming l interferences have occurred, r chips are affected with probability

$$\binom{w}{r} \binom{l-1}{r-1} / \binom{w+l-1}{w-1}$$

so up to this level, r chips are affected by at least one interference, and $w - r$ are affected by no interference. Furthermore, assuming that the desired user transmits zero, a lower bound is obtained by assuming that these r chips are affected by only one interference. An upper bound is obtained by assuming that these interfered chips are certainly (with probability 1) detected erroneously, so considering the chip-error probabilities P_0, P_1 , and P_2 defined in Section III-B, and assuming that the desired user's

$$\begin{aligned}
P_L(e|x) &= \sum_{l=0}^{N-1} \binom{N-1}{l} q^l (1-q)^{(N-1-l)} \sum_{r=1}^l \frac{\binom{w}{r} \binom{l-1}{r-1}}{\binom{w+l-1}{w-1}} \\
&\times \left(\frac{1}{2} \sum_{i=0}^r \sum_{t=\max(TH0,i)}^{w-r+i} \binom{w-r}{t-i} P_0^{t-i} (1-P_0)^{w-r-(t-i)} \binom{r}{i} P_1^i (1-P_1)^{r-i} \right. \\
&\left. + \frac{1}{2} \sum_{t=TH1}^{w-r} \binom{w-r}{t} (1-P_1)^t P_1^{w-r-t} P_2^r \right) \tag{A-5}
\end{aligned}$$

$$\begin{aligned}
P_U(e|x) &= \sum_{l=0}^{N-1} \binom{N-1}{l} q^l (1-q)^{(N-1-l)} \sum_{r=1}^l \frac{\binom{w}{r} \binom{l-1}{r-1}}{\binom{w+l-1}{w-1}} \left(\frac{1}{2} \sum_{t=\max(TH0,r)}^w \binom{w-r}{t-r} P_0^{t-r} (1-P_0)^{w-t} \right. \\
&\left. + \frac{1}{2} \sum_{i=0}^r \sum_{t=\max(TH1,i)}^{w-r+i} \binom{w-r}{t-i} (1-P_1)^{t-i} P_1^{w-r-(t-i)} \binom{r}{i} (1-P_2)^i P_2^{r-i} \right) \tag{A-6}
\end{aligned}$$

transmitted bit is zero, we can obtain the conditional error-probability bounds. For the lower bound, we have

$$\begin{aligned}
P_L(e|l, r, 0, x) &= \sum_{i=0}^r \sum_{t=\max(TH0,i)}^{w-r+i} \binom{w-r}{t-i} P_0^{t-i} \\
&\times (1-P_0)^{w-r-(t-i)} \binom{r}{i} \\
&\times P_1^i (1-P_1)^{r-i} \tag{A-1}
\end{aligned}$$

where index L represents the lower bound. In this equation, i chips of r interfered chips are detected erroneously with probability

$$\binom{r}{i} P_1^i (1-P_1)^{r-i}.$$

$w-r$ chips that are not interfered are remained. Assume that the number of total chips which are detected erroneously is t . Since i chips were detected in error, we have a total of t error chips if $t-i$ chips of $w-r$ remaining chips are detected by mistake. The probability for that equals

$$\binom{w-r}{t-i} P_0^{t-i} (1-P_0)^{w-r-(t-i)}.$$

Obviously, i can have any value between 0 and r . Also, it is obvious that $t \geq i$. The received bit will be detected by mistake only if $t \geq TH0$. Therefore, for obtaining the error probability, we must set $t \geq \max(TH0, i)$. Also noting that i chips of r interfered chips are detected by mistake, and $w-r$ chips are not interfered, it is obvious that $(w-r) + i \geq t$. The above discussion explains (A-1). Similarly, by assuming $P_1 = 1$, the upper bound is obtained as follows:

$$P_U(e|l, r, 0, x) = \sum_{i=\max(r, TH0)}^w \binom{w-r}{t-r} P_0^{t-r} (1-P_0)^{w-t}. \tag{A-2}$$

In a similar way, assuming that the desired user transmits one, since interfering signals increase the detected signal level, the upper bound is obtained by assuming that affected chips are affected with only one interference, and the lower bound is obtained by assuming that all of the affected chips are certainly detected correctly. Now, conditional probabilities can be written as

$$P_L(e|l, r, 1, x) = \sum_{t=TH1}^{w-r} \binom{w-r}{t} (1-P_1)^t P_1^{w-r-t} P_2^r \tag{A-3}$$

$$\begin{aligned}
P_U(e|l, r, 1, x) &= \sum_{i=0}^r \sum_{t=\max(TH1,i)}^{w-r+i} \binom{w-r}{t-i} \\
&\times (1-P_1)^{t-i} P_1^{w-r-(t-i)} \\
&\times \binom{r}{i} (1-P_2)^i P_2^{r-i}. \tag{A-4}
\end{aligned}$$

And finally, the upper bound and lower bound of error probability can be written as shown in (A-5)–(A-6) at the top of the page.

REFERENCES

- [1] J. Strohbehn, Ed., *Laser Beam Propagation in the Atmosphere*. New York: Springer, 1978.
- [2] J. A. Salehi, "Code-division multiple-access techniques in optical fiber networks—Part I: Fundamental principles," *IEEE Trans. Commun.*, vol. 38, no. 8, pp. 824–833, Aug. 1989.
- [3] J. A. Salehi and C. A. Brackett, "Code-division multiple-access techniques in optical fiber networks—Part II: Systems performance analysis," *IEEE Trans. Commun.*, vol. 38, no. 8, pp. 834–842, Aug. 1989.
- [4] H. M. H. Shalaby, "Chip-level detection in optical code-division multiple-access," *J. Lightw. Technol.*, vol. 16, no. 6, pp. 1077–1087, Jun. 1998.
- [5] S. Karp, R. M. Gagliardi, S. E. Moran, and L. B. Scotts, *Optical Channels, Fiber, Clouds, Water and Atmosphere*. New York: Plenum, 1980.
- [6] R. M. Gagliardi and S. Karp, *Optical Communication*, 2nd ed. New York: Wiley, 1995.
- [7] N. C. Beaulieu, A. A. Abu-Dayya, and P. J. McLane, "Estimating the distribution of a sum of independent lognormal random variables," *IEEE Trans. Commun.*, vol. 43, no. 12, pp. 2869–2873, Dec. 1995.

- [8] A. J. Viterbi, *CDMA: Principles of Spread Spectrum Communications*. Reading, MA: Addition-Wesley, 1995.
- [9] P. Azmi, M. Nasiri-Kenari, and J. A. Salehi, "Low-rate super-orthogonal channel coding for fiber-optic CDMA communication systems," *J. Lightw. Technol.*, vol. 19, no. 6, pp. 847–855, Jun. 2001.
- [10] M. Razavi and J. H. Shapiro, "Wireless optical communications via diversity reception and optical preamplification," *IEEE Trans. Wireless Commun.*, vol. 4, no. 3, pp. 975–983, May 2005.
- [11] T. Li and M. C. Teich, "Photon point process for traveling-wave laser amplifiers," *IEEE J. Quantum Electron.*, vol. 29, no. 9, pp. 2568–2578, Sep. 1993.
- [12] B. Hamzeh and M. Kavehrad, "OCDMA-coded free-space optical links for wireless optical-mesh networks," *IEEE Trans. Commun.*, vol. 52, no. 12, pp. 2165–2174, Dec. 2004.
- [13] T. Ohtsuki, "Performance analysis of atmospheric optical PPM CDMA systems," *J. Lightw. Technol.*, vol. 21, no. 2, pp. 406–411, Feb. 2003.
- [14] X. Zhu and J. M. Kahn, "Mitigation of turbulence-induced scintillation noise in free-space optical links using temporal-domain detection techniques," *IEEE Photon. Technol. Lett.*, vol. 15, no. 3, pp. 623–625, May 2003.
- [15] M. Cole and K. Kiasaleh, "Signal intensity estimators for free-space optical communications through turbulent atmosphere," *IEEE Photon. Technol. Lett.*, vol. 16, no. 6, pp. 2395–2397, Nov. 2004.



Mahmoud Jazayerifar was born in Tehran, Iran, on June 2, 1980. He received the B.S. and M.S. degrees in electrical engineering in 2002 and 2004, respectively, from Sharif University of Technology (SUT), Tehran, Iran, where he is currently working toward the Ph.D. degree in the Department of Electrical Engineering.

From June 2001 to September 2002, he was a Member of Research Staff of the Mobile Communications Division, Iran Telecommunication Research Center (ITRC), and since 2005, he has been with the Optical Network Research Lab (ONRL) as a Member of Technical Staff. His research interests include wireless communication systems and optical communication systems; specifically, optical CDMA and free-space optical systems.



Jawad A. Salehi (M'02) was born in Kazemain, Iraq, on December 22, 1956. He received the B.S. degree from the University of California, Irvine, in 1979, and the M.S. and Ph.D. degrees from the University of Southern California (USC), Los Angeles, in 1980 and 1984, respectively, all in electrical engineering.

From 1981 to 1984, he was a full-time Research Assistant with the Communication Science Institute at USC, where he was engaged in research in the area of spread-spectrum systems. From 1984 to 1993, he was a Member of Technical Staff of the Applied Research Area, Bell Communications Research (Bellcore), Morristown, NJ. From February to May 1990, he was with the Laboratory of Information and Decision Systems, Massachusetts Institute of Technology, Cambridge, as a Visiting Research Scientist conducting research on optical multiple-access networks. He was an Associate Professor from 1997 to 2003, and is currently a Full Professor, with the Electrical Engineering (EE) Department, Sharif University of Technology (SUT), Tehran, Iran. From 1999 to 2001, he was the Head of Mobile Communications Systems Group and Codirector of the Advanced and Wide-band Code Division Multiple Access (CDMA) Laboratory at Iran Telecom Research Center, Tehran, conducting research in the area of advanced CDMA techniques for optical and radio communications systems. From 2003 to 2006, he was the Director of National Center of Excellence in Communications Science at the EE department of SUT. In 2003, he founded and directed the Optical Networks Research Laboratory, Electrical Engineering Department, SUT, for advanced theoretical and experimental research in futuristic all-optical networks. He is also a Cofounder of the Advanced Communications Research Institute at SUT for advancing the graduate school research program in communications science. His current research interests include optical multiaccess networks; in particular, optical orthogonal codes, fiber-optic CDMA, femtosecond or ultrashort light pulse CDMA, spread-time CDMA, holographic CDMA, wireless indoor optical CDMA, all-optical synchronization, and applications of erbium-doped fiber amplifiers in optical systems. He is the holder of 11 U.S. patents on optical CDMA.

Dr. Salehi is a recipient of the Bellcore's Award of Excellence, the Outstanding Research Award of the EE Department of SUT in 2002 and 2003, the Outstanding Research Award of SUT 2003, the Nationwide Outstanding Research Award from the Ministry of Higher Education 2003, and the Nation's Highly Cited Researcher Award 2004. Recently, he was introduced as among the 250 preeminent and most influential researchers worldwide by the Institute for Scientific Information (ISI) Highly Cited in the computer-science category. He is the Corecipient of IEEE's Best Paper Award (on spread-time/time-hopping ultra-wideband CDMA communications systems), October 2004. He was a member of the organizing committee for the first and the second IEEE Conferences on Neural Information. Since May 2001, he has been serving as Associate Editor for optical CDMA of the IEEE TRANSACTIONS ON COMMUNICATIONS. In September 2005, he was elected as the interim Chair of the IEEE Iran section.